Acta Crystallographica Section B
Structural Science
ISSN 0108-7681

Modulated structure of potassium sodium strontium barium niobates (KNSBN): harmonic solution

Audrey Surmin,[a] Pierre Fertey,[a]* Dominik Schaniel[b] and Theo Woike[b]

[a]Laboratoire de Cristallographie et Modélisation des Matériaux Minéraux et Biologiques, UMR-CNRS-7036, Université Henri Poincaré–Nancy I, BP 239, 54 506 Vandoeuvre-lès-Nancy CEDEX, France, and [b]Institut für Mineralogie, Universität zu Köln, Zülpicher Strasse 49, D-5067 Köln, Germany

Correspondence e-mail: pierre.fertey@lcm3b.uhp-nancy.fr

Received 24 October 2005
Accepted 13 January 2006

The structures of two specimens of the $(K_{1-y}Na_y)_{2F-2}(Sr_xBa_{1-x})_{2-F}Nb_2O_6$ family (KNSBN) have been solved and refined ($x^{I} = 0.6$, $y^{I} = 0.45$, $F^{I} = 1.07$ and $x^{II} = 0.72$, $y^{II} = 0.45$, $F^{II} = 1.08$). The KNSBN compounds appear to be incommensurately modulated, as described in a five-dimensional superspace approach with the tetragonal $P4bm$ ($pp1/2$, $p - p1/2$) superspace group. Their modulation wavevectors are almost independent of the composition. The description of the modulation is restricted to first-order harmonics in order to limit the number of refined parameters. The modulation mainly affects the positions of the O atoms and their displacements depend on the Sr/Ba ratio. The structural models for the two compounds are not only almost identical, but also analoguous to the structural model of the $Sr_xBa_{1-x}Nb_2O_6$ parent compound: doping with K^+ and Na^+ cations has no significant influence on the incommensurate modulation, contrary to the strong dependence observed for the physical properties.

1. Introduction

The photorefractive properties of oxidic materials have been a subject of great interest in recent years owing to the potential applications in optical information processing, such as volume holographic data storage, coherent light amplification, optical phase conjugation, optical communication, optical interconnects and optical computing (Coufal *et al.*, 2000). Among ferroelectric materials, a number of ferroelectric compounds which crystallize with a tungsten-bronze (TB)-type structure in the tetragonal or orthorhombic symmetry are particularly promising, *e.g.* $Sr_xBa_{1-x}Nb_2O_6$ and $Ba_2NaNb_5O_{15}$.

The tungsten-bronze-type structure can be considered as a framework of corner-sharing oxygen octahedra, as illustrated in Fig. 1, forming three types of interstitials (C, $A1$ and $A2$) which may receive different cations and which can be either partially filled or fully occupied by different cations. The physical properties may be varied significantly by doping or substituting with the desired cation impurities in these intersitials (Xu, 1991). A series of experiments has been carried out on $Sr_xBa_{1-x}Nb_2O_6$ (SBN) to improve its crystal properties. Among them, the potassium and sodium (K/Na) modified SBN, *i.e.* $(K_{1-y}Na_y)_{2F-2}(Sr_xBa_{1-x})_{2-F}Nb_2O_6$ (KNSBN, filling factor F, $0.25 \leq y \leq 0.5$, $0.25 \leq x \leq 0.75$), have been reported to have high electro-optic coefficients, a large transparent range, a high threshold energy for optical damage and a Curie temperature above 473 K, suitable for many optical device applications (Tomita *et al.*, 1993; Shen *et al.*, 1999; Xia *et al.*,

1998). The temperature range of the ferroelectric relaxor-type phase transition can be controlled by the compositions x and y (Xu *et al.*, 1984). Surprisingly, no structural analysis of KNSBN has been reported until now.

SBN belongs to the partially filled TB type (Jamieson *et al.*, 1968). Several studies have shown that the C site is empty and five of the six A sites are occupied: $A1$ sites are exclusively occupied by Sr cations with an average filling of 70%, depending on the exact composition. The $A2$ sites can be occupied by Sr or Ba cations (Chernaya *et al.*, 1997). It is generally admitted that introducing K^+ and Na^+ in the crystal leads to the occupation of $A1$ and $A2$ cavities, depending on the filling factor F which varies between $1 \leq F \leq 1.2$ so that $A1$ and $A2$ are totally filled for $F = 1.2$. The C cavities remain empty as they are too small to be occupied by K^+ or Na^+. The filling of empty $A1$ and $A2$ sites with K^+ and Na^+ is expected to influence or even suppress the disorder and incommensurate modulation observed in pure SBN (Schneck *et al.*, 1981; Bursill & Lin, 1987; Prokert *et al.*, 1991; Woike *et al.*, 2003). Therefore, we have extended our structural investigations from SBN to KNSBN. Here we present the average structure and the incommensurate modulation of two KNSBN single crystals with different Sr content, x. The results are compared with the pure SBN crystals. We show that the incorporation of Na and K into SBN does not eliminate the incommensurate modulation.

2. Experimental

All single crystals were grown by the Czochralski method. The composition was checked by X-ray fluorescence analysis. The compositions were found to be $K_{0.08\ (2)}Na_{0.07\ (2)}Sr_{0.56\ (1)}Ba_{0.38\ (1)}Nb_{1.99\ (1)}O_6$ for the first sample, which is close to $(K_{0.55}Na_{0.45})_{0.13}(Sr_{0.60}Ba_{0.40})_{0.93}Nb_2O_6$ (KNSBN60) with $x = 0.60$, $y = 0.45$ and $F = 1.07$. The composition of the second one was $K_{0.09\ (2)}Na_{0.08\ (2)}Sr_{0.67\ (1)}Ba_{0.26\ (1)}Nb_{1.99\ (1)}O_6$, which can be approximated by $(K_{0.55}Na_{0.45})_{0.15}(Sr_{0.72}Ba_{0.28})_{0.92}Nb_2O_6$ (KNSBN72) with $x = 0.72$, $y = 0.45$ and $F = 1.08$. The samples were mechanically ground to the shape of spheres and were not polarized to ferroelectric single domain crystals before the X-ray study, so antiparallel domains were present.

The data were collected on a Enraf–Nonius KappaCCD four-circle diffractometer (see Table 1 for experimental details[1]). The image processing was performed using the *Evalccd* software package (Duisenberg *et al.*, 2003). All the reflections observed were indexed by five integer indices, *hklmn*, with respect to the five-dimensional base (de Wolff, 1974). Only the first-order satellites (*hkl* ± 10 or *hkl*0 ± 1) could be detected and integrated.

The structure refinement was performed using *JANA*2000 (Petricek *et al.*, 2000). The modulated structure of SBN61 proposed by Woike *et al.* (2003) and Schaniel *et al.* (2002) was taken as the starting model. Considering the ionic radii of the K and Na cations, the smaller Na cations were supposed to exclusively occupy the $A1$ sites, whereas the K cations were restricted to the $A2$ sites. The C site was kept empty. Only harmonic modulation functions of the two wavevectors $\mathbf{q}_k$ ($k = 1, 2$) were used. The modulation parameter p_i describing the displacive, occupation or thermal parameter waves is a periodic function of the actual position in the crystal $(\mathbf{x}_0 + \mathbf{n})$ and is written as

$$p_i = \sum_k U^i_{s,k} \sin\left[2\pi\mathbf{q}_k \cdot (\mathbf{x}_0 + \mathbf{n})\right] + U^i_{c,k} \cos\left[2\pi\mathbf{q}_k \cdot (\mathbf{x}_0 + \mathbf{n})\right],$$

where $U^i_{s,k}$ and $U^i_{c,k}$ are the amplitudes of the harmonic waves.

3. Results and discussion

The compositions deduced from the X-ray fluorescence analysis imply that the $A1$ and $A2$ channels cannot be simultaneously filled (filling factor of 1.07 for both samples).

The diffraction images unambiguously showed the presence of additional reflections located in the plane perpendicular to the polar axis at $l = 2n + 1$, as observed for the parent SBN compounds. The cell parameters and the two modulation vector components were refined using all the reflections. As reported in Table 1, the cell parameters decrease when the concentration in Sr increases, as generally observed in the SBN family: this is to be related to the average size of the $A2$ site which should decrease when the Ba content diminishes (steric effect of Ba). The modulation vectors are only slightly affected by the composition of the sample, as previously observed in the parent family (Savenko *et al.*, 1990).

In a first refinement (initial model), all the atomic proportions were set to the values deduced from the X-ray fluores-

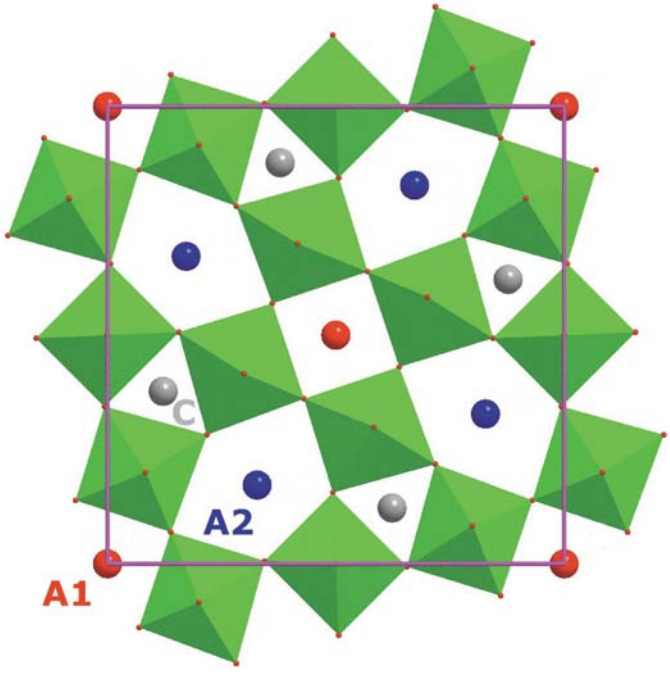

Figure 1
Projection in the (001) plane of the SBN average structure.

[1] Supplementary data for this paper are available from the IUCr electronic archives (Reference: CK5014). Services for accessing these data are described at the back of the journal.

Table 1
Experimental details.

	KNSBN60 (I)	KNSBN72 (II)
Crystal data		
Chemical formula	$Ba_{0.38}K_{0.085}Na_{0.07}Nb_2O_6Sr_{0.56}$	$Ba_{0.26}K_{0.096}Na_{0.08}Nb_2O_6Sr_{0.676}$
M_r	388	382.3
Cell setting, space group	Tetragonal, *X*4*bm*	Tetragonal, *X*4*bm*
Temperature (K)	293	293
a, *c* (Å)	12.4375 (5), 7.8807 (2)	12.4292 (8), 7.8524 (3)
V (Å^3)	1219.08 (8)	1213.08 (12)
Z	10	10
D_x (Mg m^{-3})	5.283	5.221
Radiation type	Mo *K*α	Mo *K*α
No. of reflections for cell parameters	4101	2000
θ range (°)	3.04–59.63	3.28–40.46
μ (mm^{-1})	13.79	14.11
Crystal form, colour	Sphere, transparent	Sphere, transparent
Crystal radius (mm)	0.078	0.117
Data collection		
Diffractometer	Nonius CCD	Nonius CCD
Data collection method	ω scan, integration method	ω scan, integration method
Absorption correction	Sphere	Sphere
T_{min}	0.221	0.106
T_{max}	0.288	0.152
No. of measured, independent and observed reflections	144 596, 8612, 7718	96 783, 7577, 6196
Criterion for observed reflections	$I>3\sigma(I)$	$I>3\sigma(I)$
R_{int}	0.038	0.038
θ_{max} (°)	59.6	40.5
Range of *h*, *k*, *l*, *m*, *n*	$-27 \Rightarrow h \Rightarrow 29$ $-30 \Rightarrow k \Rightarrow 28$ $-18 \Rightarrow l \Rightarrow 18$ $-1 \Rightarrow m \Rightarrow 1$ $-1 \Rightarrow n \Rightarrow 1$	$-22 \Rightarrow h \Rightarrow 22$ $-22 \Rightarrow k \Rightarrow 19$ $-14 \Rightarrow l \Rightarrow 14$ $-1 \Rightarrow m \Rightarrow 1$ $-1 \Rightarrow n \Rightarrow 1$
Refinement		
Refinement on	*F*	*F*
$R[F^2 > 2\sigma(F^2)]$, $wR(F^2)$, *S*	0.051, 0.087, 2.61	0.055, 0.074, 2.32
No. of reflections	8612	6196
No. of parameters	150	129
Weighting scheme	Based on measured s.u.s, $w = 1/[\sigma^2(F) + 0.0004F^2]$	Based on measured s.u.s, $w = 1/[\sigma^2(F) + 0.0004F^2]$
$(\Delta/\sigma)_{max}$	0.026	0.006
$(\Delta\rho)_{max}$, $(\Delta\rho)_{min}$ (e Å^{-3})	3.64, −5.83	3.07, −5.07
Extinction method	B–C type 1 Lorentzian isotropic (Becker & Coppens, 1974)	B–C type 1 Lorentzian isotropic (Becker & Coppens, 1974)
Extinction coefficient	0.058 (4)	0.069 (3)

Symmetry codes of the five-dimensional space group: $x_1\ x_2\ x_3\ x_4\ x_5$; $-x_2\ x_1\ x_3\ x_5\ -x_4$; $\frac{1}{2}-x_1\ \frac{1}{2}+x_2\ x_3\ -x_5\ -x_4$; $-x_1\ -x_2\ x_3\ -x_4\ -x_5$; $\frac{1}{2}-x_2\ \frac{1}{2}-x_1\ x_3\ -x_4\ x_5$; $x_2\ -x_1\ x_3\ -x_5\ x_4$; $\frac{1}{2}+x_1\ \frac{1}{2}-x_2\ x_3\ x_5\ x_4$; $\frac{1}{2}+x_2\ \frac{1}{2}+x_1\ x_3\ x_4\ -x_5$. Computer programs used: *JANA*2000 (Petricek *et al.*, 2000).

cence analysis: the Sr occupancies in the *A*1 and *A*2 channels were constrained in order to keep constant the total amount of Sr in the cell. Pseudo-atoms composed of Sr and Na on the one hand and Sr, K and Ba on the other hand were placed at the *A*1 and *A*2 channel sites, respectively. Unique positions, and displacement and modulation parameters were refined for each pseudo-atom. The refinement of the average structure parameters and the positional modulation parameters converged smoothly. The *R* values are reported in Table 2. It can be seen that the residues for the satellite reflections reached about 20% at this stage. As observed in SBN61, residual electron-density maps at the *A*2 sites revealed large maxima and minima. Their positions depend on the internal coordinates x_4 and x_5. As already observed in SBN61, neither different split-atom models (where the parameters of K, Sr and Ba are refined independently) nor an occupational modulation of the *A*2 sites gave satisfactory results: in each case, strong correlation coefficients were observed between the K, Sr or Ba parameters. The additional distribution of the electronic density at this site was therefore described as a modulation of the displacement parameters of the *A*2 pseudo-atom. The residues for the satellites reflections dropped immediately (*cf.* Table 2).

3.1. Averaged structure

The average structures of KNSBN60 and KNSBN72 are highly consistent with the usual structural model of the SBN family (Chernaya *et al.*, 1997, 2000; Woike *et al.*, 2003), as reported in Tables 3 and 4, respectively. The large values of the isotropic displacement parameters for the O atoms and for the pseudo-atom (Ba/Sr/K) at the *A*2 site reflect the structural distortion induced by the different types of atom that can occupy this site. This effect is less pronounced for the pseudo-atom (Sr/Na) at the *A*1 site. For the KNSBN60 sample, the anisotropic displacement parameters of the O atoms could be refined. The anisotropic displacement parameters are reported in Table 5. The ellipsoids describing the anisotropic vibrations of the O4 and O5 atoms are flattened in a plane perpendicular to the polarization direction. This is a consequence of the steric effect of the different atoms at the *A*1 or *A*2 sites, inducing a static/dynamic structural disorder of the apical oxygen of the NbO_6 octahedra. The vibrations of the cations are almost isotropic, except for the pseudo-atom at the *A*2 site: its ellipsoid is also slightly flattened in a plane perpendicular to the polar axis.

It can be noticed that the filling of the *A*1 sites is almost constant for the two samples: since the Na concentrations are different, the proportion of Sr is adjusted so that the *A*1 site-occupancy reaches $\sim 91\%$ for both compounds. This seems to be a common trend for the different members of the KNSBN or SBN family (Chernaya *et al.*, 1997). Since the filling factors

Table 2
Residues for all, main and satellites reflections for the initial (*i.e.* no modulation of the displacement parameters for the *A*2 pseudo-atom) and final structural models.

	KNSBN60			KNSBN72		
	R_{all}	R_{main}	R_{sat}	R_{all}	R_{main}	R_{sat}
Initial	0.0684	0.0455	0.2326	0.0875	0.0450	0.2149
Final	0.0506	0.0392	0.1322	0.0548	0.0303	0.1286

Table 3
Fractional atomic coordinates and isotropic displacement parameters (Å^2) for the averaged structure of KNSBN60.

Pseudo-atoms *A*1 = 73.0 (3)% Sr + 17.5% Na and *A*2 = 41.1 (7)% Sr + 40.3 (6)% Ba + 10.6% K.

Atom	Site occupancy	*x*	*y*	*z*	U_{iso} ($\times 10^3$)
Nb1	1	0	0.5	0.00125 (9)	6.10 (5)
Nb2	1	0.074775 (15)	0.211720 (14)	−0.00588 (8)	6.91 (4)
*A*1	0.905 (3)	0	0	0.23884 (11)	7.07 (9)
*A*2	0.92	0.17168 (2)	0.67168 (2)	0.2404	21.87 (7)
O1	1	0.34344 (15)	0.00549 (16)	−0.0262 (4)	11.8 (4)
O2	1	0.13858 (17)	0.06904 (14)	−0.0287 (3)	10.7 (4)
O3	1	0.28172 (16)	0.78172 (16)	−0.0229 (4)	10.0 (4)
O4	1	0	0.5	0.2307 (6)	19.0 (8)
O5	1	0.29600 (16)	0.42432 (15)	0.2273 (3)	12.6 (5)

Table 4
Fractional atomic coordinates and isotropic displacement parameters (Å^2) for KNSBN72.

Pseudo-atoms *A*1 = 71.2 (4)% Sr + 19.7% Na and *A*2 = 56.0 (8)% Sr + 24.7 (8)% Ba + 12% K.

Atom	Site occupancy	*x*	*y*	*z*	U_{iso} ($\times 10^3$)
Nb1	1	0	0.5	0.00128 (12)	7.38 (8)
Nb2	1	0.074907 (18)	0.211795 (17)	−0.00681 (10)	8.31 (6)
*A*1	0.909 (4)	0	0	0.23820 (13)	7.45 (13)
*A*2	0.927 (8)	0.17129 (3)	0.67129 (3)	0.240438	25.74 (9)
O1	1	0.34394 (15)	0.00525 (14)	−0.0263 (3)	9.0 (3)
O2	1	0.13855 (16)	0.06807 (15)	−0.0286 (3)	10.6 (3)
O3	1	0.28142 (15)	0.78142 (15)	−0.0207 (4)	9.3 (4)
O4	1	0	0.5	0.2334 (7)	18.4 (8)
O5	1	0.29630 (13)	0.42457 (15)	0.2277 (3)	9.1 (4)

Table 5
Anisotropic displacement parameters ($\times 10^3$) for the KNSBN60 sample at room temperature.

Atom	U^{11}	U^{22}	U^{33}	U^{23}	U^{13}	U^{12}
Nb1	6.49 (8)	6.49 (8)	5.33 (12)	−0.17 (8)	0	0
Nb2	7.27 (7)	6.25 (6)	7.20 (7)	0.83 (4)	0.20 (8)	−1.46 (8)
*A*1	6.84 (12)	6.84 (12)	7.5 (2)	0	0	0
*A*2	26.41 (11)	26.41 (11)	12.78 (14)	−16.50 (14)	−0.53 (10)	−0.53 (10)
O1	6.3 (5)	14.8 (7)	14.4 (9)	−4.0 (5)	−1.9 (8)	3.2 (8)
O2	17.2 (8)	6.8 (6)	8.2 (9)	6.2 (5)	−1.1 (7)	−3.4 (6)
O3	9.8 (5)	9.8 (5)	10 (1)	3.2 (6)	3.7 (7)	3.7 (7)
O4	26 (1)	26 (1)	5 (1)	5 (1)	0	0
O5	19 (1)	19 (1)	3.4 (8)	−3.0 (7)	0.7 (6)	−1.4 (8)

for these two samples are almost identical, it is not surprising that the filling of the *A*2 channel is also identical ($\sim$ 92%). Therefore, one can conclude that the Sr cations preferentially filled the *A*1 site up to the optimal value. The *A*2 site is then filled with surplus Sr and the other cations (Ba, K).

Bond-valence sums were used to check the initial Na, K and C site hypothesis. Table 6 reports the calculated bond values. For both cations, the expected bond-valence value should be around 1. From Table 6, it becomes clear that K cannot occupy the *A*1 or the C sites since the bond sums greatly exceed the expected ones. On the other hand, acceptable bond sums are calculated for the *A*2 sites for both compounds. For the same reasons, C sites cannot be filled with Na atoms. Bond sums are, however, compatible with an occupancy of both the *A*1 and *A*2 sites with Na. Supposing that the *A*1 sites are always preferentially filled before the *A*2 sites, the Na atoms should therefore predominantly occupy the *A*1 sites.

Considering the lower accuracy of the Na and K concentrations deduced from the X-ray fluorescence analysis (within 15%), we tried a refinement where the *A*1 and *A*2 channels were completely filled with Na and K cations, respectively. The final residues were slightly increased. For KNSBN60, the refined Na concentration (*i.e.* 0.45 Na atom per unit cell) gave about 30% extra Na compared with the X-ray fluorescence results (0.35 atoms per unit cell). The refined K concentrations (0.83 atom per unit cell) was much larger than the fluorescence results (0.42 atom per unit cell). On the contrary, releasing the filling constraint for each channel, the proportions of K and Na were refined. The concentrations of Na and K were, however, kept equal. This led to significantly lower and unacceptable concentrations (0.11 atom per unit cell), although the residues of the refinement were slightly improved. Analogous results were obtained for KNSBN72. The poor accuracy of the refined Na and K concentrations is related to the difficulty in separating the contributions originating from the disordered nature of the structure (partial site occupancy by atoms with different atomic numbers), the low cell content of Na and K atoms, and the presence of incommensuration. Therefore, in our final model the Na and K concentrations were kept fixed to the X-ray fluorescence results. The constraint on the Sr content of the *A*1 and *A*2 sites was released. The proportions of Sr atoms with respect to Ba atoms were constrained to

a value deduced from the X-ray fluorescence analysis. The final residues are reported in Table 2. The modulation parameters of this latter structural model and their comparison with the parent SBN61 compound will now be detailed.

3.2. Modulated structure

Table 7 details the most significant modulation parameters. In this table the parameters of the parent compound SBN61 are also reported. The modulated structures of KNSBN60 and KNSBN72 are similar to the modulated structure of SBN61. Considering the atomic position modulations, the amplitudes of the O-atom functions are the most significant compared with the amplitudes for the cations. The modulation parameters of the O atoms are about 10 times stronger than the amplitudes of the $A2$ pseudo-atom. Niobium and $A1$ pseudo-atom positions are only slightly modulated. The basal O atoms of the NbO_6 octahedra have a displacement modulation mainly along the c axis. On the contrary, the displacements of the apical oxygen are perpendicular to the polar axis. This is illustrated in Fig. 2 where the modulation functions for the z and x coordinates of the O atoms of the Nb(1)O_6 tetrahedron are plotted. Since the amplitudes of the modulation functions of the O atoms are similar (amplitude ~ 0.2 Å), the NbO_6 octahedra can therefore be considered as more or less rigid units precessing around the polar axis.

Table 6
Bond-valence sums for the K and Na cations.

	Minimum	Maximum	Average
KNSBN60			
K at $A1$	2.35 (7)	2.48 (7)	2.43 (1)
K at C	4.03 (7)	5.00 (7)	4.41 (7)
K at $A2$	1.22 (7)	1.57 (7)	1.38 (7)
Na at C	1.65 (7)	2.05 (7)	1.81 (7)
Na at $A2$	0.96 (7)	1.02 (7)	0.99 (7)
Na at $A1$	0.50 (7)	0.64 (7)	0.57 (7)
KNSBN72			
K at $A1$	2.24 (7)	2.44 (7)	2.37 (1)
K at C	4.27 (7)	5.67 (7)	4.80 (7)
K at $A2$	1.22 (7)	1.71 (7)	1.44 (7)
Na at C	1.62 (7)	2.16 (7)	1.83 (7)
Na at $A2$	0.46 (7)	0.65 (7)	0.55 (7)
Na at $A1$	0.85 (7)	0.93 (7)	0.90 (7)

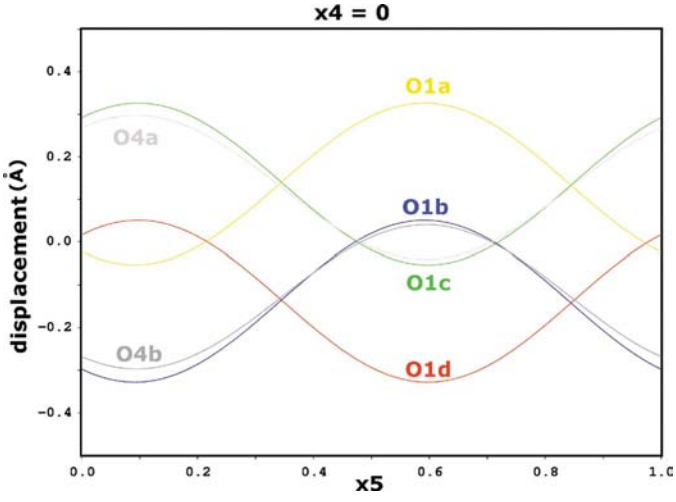

Figure 2
x and z displacement functions of O1 (basal) and O4 (apical) atoms for the Nb(1)O_6 octahedra.

As already observed for the parent compound, the ellipsoids that describe anisotropic vibrations of the $A2$ pseudo-atom are strongly modulated (*cf.* Table 8): they are flattened in the xy plane and their long axis direction is correlated with the geometrical distortion induced by the modulated displacements of the apical O4 and O5 O atoms. These modulated ellipsoids are introduced to model physically different phenomena that cannot be distinguished by our lack of resolution: displacement and/or occupation modulations; different behaviors for the different species at the $A2$ site (with different scattering power). The description of the modulation should be improved since the calculated electronic residual density maps at this site show some residues. The measurements of high-order $(m, n>1)$ and mixed satellites ($hkl \pm 1 \pm 1$) could help to go beyond a simple harmonic approximation.

More interesting is the comparison of the modulation parameters between the two compositions. Significant differences appear for the O atoms: the average amplitude of the cosine and sine waves of KNSBN72 are $\sim 25\%$ larger than those of KNSBN60. Although less significant, the same tendency is observed for

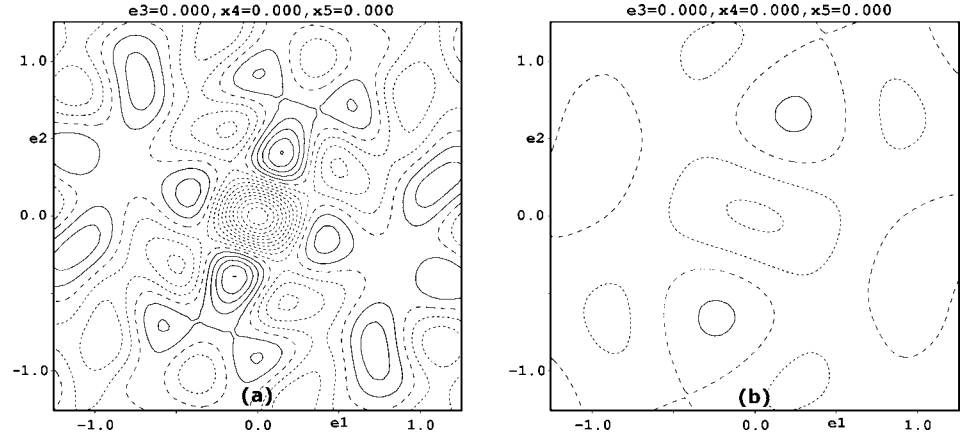

Figure 3
Residual density maps at the O4 site for KNSBN60: (*a*) full data set and (*b*) truncated data set ($\sin\theta/\lambda < 0.6$ Å^{-1}), contour 0.5 e Å^{-3}.

Table 7
Most significant displacement parameters ($\times 10^2$).

			KNSBN60		KNSBN72		SBN61	
Atom	Axe	q	cos	sin	cos	sin	cos	sin
O1	z	1	0.59 (3)	2.03 (3)	0.74 (3)	2.57 (3)	0.59 (4)	2.13 (4)
O1	z	2	−0.79 (3)	−2.28 (3)	−0.81 (3)	−3.06 (3)	−0.73 (4)	−2.30 (4)
O2	z	1	1.33 (3)	1.55 (3)	1.44 (3)	2.16 (3)	1.14 (3)	1.61 (4)
O2	z	2	−1.85 (3)	0.76 (3)	−2.30 (3)	0.88 (3)	−1.79 (4)	0.82 (3)
O3	z	1	−1.30 (3)	−0.77 (3)	−1.84 (4)	−1.19 (4)	−1.25 (4)	−0.83 (4)
O3	z	2	1.12 (3)	0	1.70 (4)	0	1.25 (4)	0
O4	x	1	0	−1.36 (3)	0	−1.82 (3)	0	−1.34 (4)
O4	y	1	0	−1.36 (3)	0	−1.82 (3)	0	−1.34 (4)
O4	x	2	0	1.24 (3)	0	1.22 (3)	0	1.36 (4)
O4	y	2	0	−1.24 (3)	0	−1.22 (3)	0	−1.36 (4)
O5	x	1	−0.195 (16)	1.049 (17)	−0.242 (16)	1.273 (16)	−0.18 (2)	1.11 (2)
O5	y	1	1.284 (19)	−0.672 (19)	1.675 (19)	−0.82 (2)	1.37 (3)	−0.74 (3)
O5	x	2	0.422 (17)	−0.571 (16)	0.566 (17)	−0.645 (17)	0.46 (2)	−0.62 (2)
O5	y	2	−1.29 (2)	1.265 (19)	−1.593 (19)	1.68 (2)	−1.32 (3)	1.41 (3)
*A*1	x	1	0	0.018 (3)	0	0.026 (3)	0	0.017 (5)
*A*1	y	1	0	0.038 (3)	0	0.047 (3)	0	0.026 (5)
*A*1	z	1	−0.014 (7)	0	−0.022 (7)	0	−0.009 (11)	0
*A*1	x	2	0	0.038 (3)	0	0.047 (3)	0	0.026 (5)
*A*1	y	2	0	−0.018 (3)	0	−0.026 (3)	0	−0.017 (5)
*A*1	z	2	−0.014 (7)	0	−0.022 (7)	0	−0.009 (11)	0
*A*2	x	1	0.0700 (17)	0.0967 (18)	0.108 (2)	0.140 (2)	0.083 (2)	0.117 (3)
*A*2	y	1	0.0700 (17)	0.0967 (18)	0.108 (2)	0.140 (2)	0.083 (2)	0.117 (3)
*A*2	z	1	0.147 (7)	−0.132 (6)	0.343 (7)	−0.242 (7)	0.217 (9)	−0.225 (9)
*A*2	x	2	−0.1487 (19)	0.534 (3)	−0.195 (2)	0.694 (4)	−0.166 (3)	0.583 (4)
*A*2	y	2	−0.1487 (19)	−0.534 (3)	−0.195 (2)	−0.694 (4)	−0.166 (3)	−0.583 (4)
*A*2	z	2	−0.061 (7)	0	−0.037 (7)	0	−0.065 (9)	0
Nb1	x	1	0	−0.102 (3)	0	−0.164 (3)	0	−0.114 (5)
Nb1	y	1	0	−0.102 (3)	0	−0.164 (3)	0	−0.114 (5)
Nb1	x	2	0	0.077 (3)	0	0.116 (3)	0	0.073 (5)
Nb1	y	2	0	−0.077 (3)	0	−0.116 (3)	0	−0.073 (5)
Nb2	x	1	−0.124 (2)	−0.067 (2)	−0.154 (2)	−0.082 (2)	−0.114 (4)	−0.060 (4)
Nb2	y	1	0.045 (2)	0.076 (3)	0.056 (2)	0.106 (2)	0.065 (4)	0.069 (4)
Nb2	x	2	0.118 (3)	−0.074 (3)	0.136 (2)	−0.106 (2)	0.112 (4)	−0.086 (4)
Nb2	y	2	−0.058 (2)	0.035 (3)	−0.041 (2)	0.051 (2)	−0.061 (4)	0.027 (4)

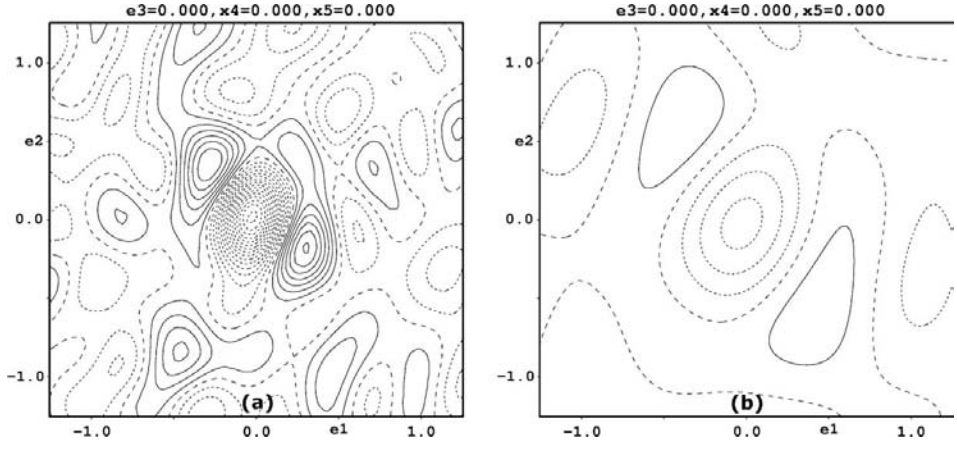

Figure 4
Residual density maps at the O5 site for KNSBN60: (*a*) full data set and (*b*) truncated data set ($\sin\theta/\lambda < 0.6$ Å^{-1}), contour 0.5 e Å^{-3}.

the parameters of the *A*2 pseudo-atoms. A comparable evolution is also observed for the amplitudes of the anisotropic modulation displacement parameters at the *A*2 site. The increase of these amplitudes for the KNSBN72 with respect to those of the KNSBN60 is even more pronounced ($\sim 60\%$). These evolutions shoud be attributed to the increase of the structural distortion induced by the different Sr(Ba) concentrations in the unit cell, particularly at the *A*2 site. The ionic radii of the Sr and Ba cations indeed are quite different.

Table 8
Displacement modulation parameters of the $A2$ pseudo-atom ($\times 10^2$).

		U^{11}	U^{22}	U^{33}	U^{12}	U^{13}	U^{23}
KNSBN60							
		2.641 (11)	2.641 (11)	1.278 (14)	−1.650 (14)	−0.053 (10)	−0.053 (10)
cos	1	−0.545 (12)	−0.545 (12)	−0.140 (19)	0.309 (15)	0.051 (13)	0.051 (13)
sin	1	−0.744 (12)	−0.744 (12)	−0.135 (18)	0.708 (15)	0.027 (13)	0.027 (13)
cos	2	0.889 (12)	0.889 (12)	0.193 (18)	−0.697 (15)	−0.068 (12)	−0.068 (12)
sin	2	−0.872 (14)	0.872 (14)	0	0	0.051 (17)	−0.051 (17)
KNSBN72							
		3.204 (13)	3.204 (13)	1.31 (2)	−2.14 (2)	0.100 (15)	0.100 (15)
cos	1	−0.890 (14)	−0.890 (14)	−0.19 (2)	0.599 (17)	0.063 (12)	0.063 (12)
sin	1	−1.453 (16)	−1.453 (16)	−0.14 (2)	1.362 (19)	−0.077 (12)	−0.077 (12)
cos	2	1.438 (15)	1.438 (15)	0.34 (2)	−1.290 (19)	0.021 (13)	0.021 (13)
sin	2	−1.199 (16)	1.199 (16)	0	0	0.068 (18)	−0.068 (18)
SBN61							
		2.782 (16)	2.782 (16)	1.39 (2)	−1.70 (2)	−0.037 (18)	−0.037 (18)
cos	1	−0.430 (16)	−0.430 (16)	−0.17 (2)	0.261 (19)	0.111 (16)	0.111 (16)
sin	1	−0.949 (17)	−0.949 (17)	−0.01 (2)	0.91 (2)	−0.049 (16)	−0.049 (16)
cos	2	0.905 (16)	0.905 (16)	0.23 (2)	−0.77 (2)	−0.014 (16)	−0.014 (16)
sin	2	−0.940 (19)	0.940 (19)	0	0	−0.13 (2)	0.13 (2)

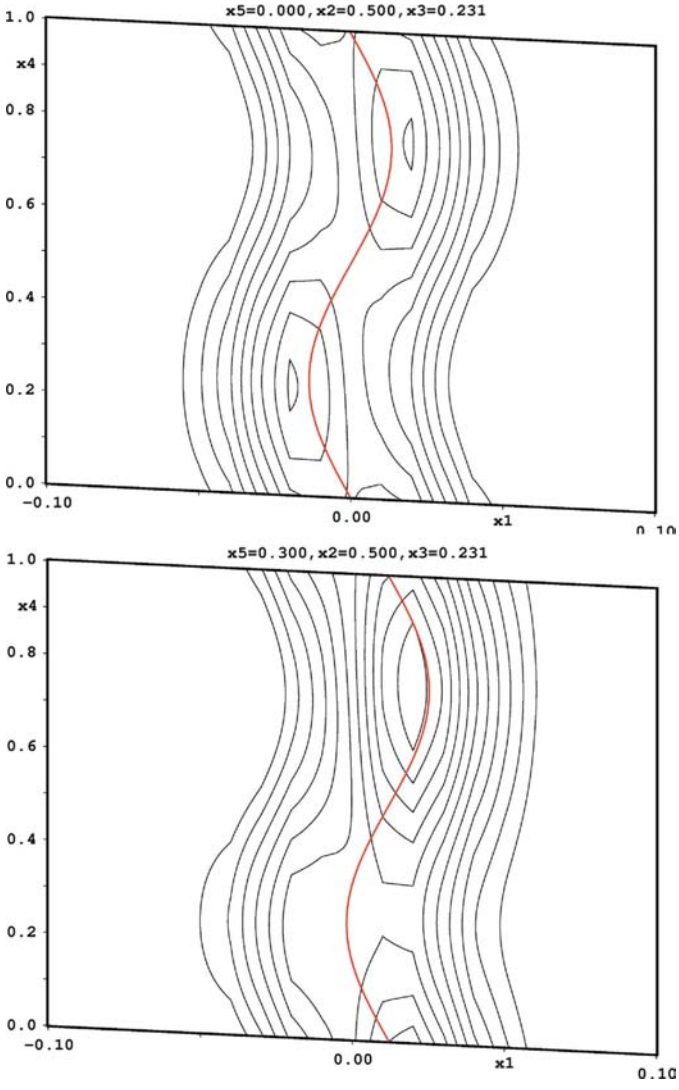

Figure 5
$x_1 - x_4$ sections of the electron density at the O4 site for KNSBN60 at $x_5 = 0.0$ and $x_5 = 0.3$.

Therefore, when the Sr(Ba) proportions of the $A2$ pseudo-atom are significantly increased (decreased) from 41% (40.3%) to 56% (24.7%) going from KNSBN60 to KNSBN72, it increases the structural distortion.

We note that the KNSBN60 and SBN61 structural models are almost identical. The amplitudes of the modulation parameters of the anisotropic vibrations are, however, slightly different: considering the influence of the Sr content of the cell on the displacement parameters rather than on the displacement parameters, the slightly different concentrations between KNSBN60 and SBN61 might explain the only slightly larger values for the SBN61 compound. Thus, doping with K^+ and Na^+ cations seems to have no significant influence on the incommensurate modulation.

Consequently, a comparison between the structural models of SBN61 and KNSBN60 shows that the origin of the variation of the physical properties, *e.g.* the increase of the ferroelectric phase transition temperature from *ca* 353 K in SBN61 to *ca* 473 K in KNSBN61, is not related to the incommensurations. The modulation appears as a consequence of the distortion of the $A2$ site depending on its content: the higher the Sr/Ba ratio, the stronger the amplitude of the modulation. In that context, the relevance of the K/Na substitutions is limited [at least, as long as the (ionic) radius of the substituants are smaller than the (ionic) radius of Ba or Sr].

3.3. Open questions

As revealed by the Fourier difference maps the refined model for the modulation describes the structure with reasonably good precision and the main features of the modulation can clearly be deduced. However, the Fourier difference maps also indicate some residues at the positions of the O4 and O5 atoms. These residues appear only when taking into account the full data set up to $\sin\theta/\lambda = 1.2$ Å^{-1}. Cutting the data analysis at $\sin\theta/\lambda = 0.6$ Å^{-1} the refined model matches very well (see Figs. 3 and 4). Neither a refinement of their site occupancy nor an anharmonic description of their thermal vibrations were able to reduce these observed residues. A modulation of the displacement parameters of the O4 and O5 atoms was also unsuccessful in describing this extra density. Furthermore, since the harmonic model uses two waves that have arguments, x_4 and x_5, respectively, the modulation function should have a constant shape as a function of $x_4(x_5)$ for any fixed value of $x_5(x_4)$. Fig. 5 displays $x_1 - x_4$ sections of the electron density map through the atomic position of O4 for $x_5 = 0$ and for $x_5 = 0.3$. The function shape is clearly dependent on the x_5 argument which assesses the limit of the harmonic model. A more complex structural model, including higher harmonic modulation

functions, could help to improve the refinement. For this purpose the measurements of high order and/or mixed satellites is also necessary.

4. Conclusions

We have solved the structures of $K_{0.08}Na_{0.07}Sr_{0.56}Ba_{0.38}Nb_2O_6$ [KNSBN60 (I)] and $K_{0.09}Na_{0.08}Sr_{0.67}Ba_{0.26}Nb_2O_6$ [KNSBN72 (II)] as incommensurate structures in five-dimensional superspace in the harmonic approximation. The results show that doping with K^+ and Na^+ cations has no significant influence on the incommensurate modulation compared with the undoped SBN compounds. Hence, the influence of these cations on the ferroelectric properties is not connected to the incommensurate modulation of the structure. As in the case of the undoped SBN61 the harmonic analysis based on first-order satellites describes the main features of the modulated structure. However, the data collection up to high angles reveals some features which cannot be explained within this harmonic picture. A more sophisticated analysis including a non-harmonic approach can only be done if the intensities of higher-order satellites, which can only be measured with high intensity X-ray sources, are available.

References

Becker, P. J. & Coppens, P. (1974). *Acta Cryst.* A**30**, 129–153.
Bursill, L. & Lin, P. J. (1987). *Acta Cryst.* B**43**, 49–56.
Chernaya, T., Maksimov, B., Verin, I., Ivleva, L. & Simonov, V. (1997). *Cryst. Rep.* **42**, 375–380.
Chernaya, T., Maksimov, B., Volk, T., Ivleva, L. & Simonov, V. (2000). *Phys. Solid State*, **42**, 1716–1721.
Coufal, H., Psaltis, D. & Sincerbox, G. (2000). *Holographic Data Storage.* Berlin: Springer.
Duisenberg, A., Kroon-Batenburg, L. M. J. & Schreurs, A. M. M. (2003). *J. Appl. Cryst.* **36**, 220–229.
Jamieson, P., Abrahams, S. & Berstein, J. (1968). *J. Chem. Phys.* **48**, 5048–5057.
Petricek, V., Dusek, M. & Palatinus, L. (2000). *JANA*2000. Technical Report. Institute of Physics, Praha, Czech Republic.
Prokert, F., Sangaa, D. & Savenko, B. (1991). *Ferroelectr. Lett.* **13**, 61–66.
Savenko, B., Sangaa, B. & Prokert, F. (1990). *Ferroelectrics*, **107**, 207–212.
Schaniel, D., Schefer, J., Petricek, V., Imlau, M., Pankrath, R., Granzow, T. & Woike, T. (2002). *Appl. Phys. A*, **74**, S963–S965.
Schneck, J., Toledano, J., Whatmore, R. & Ainger, F. (1981). *Ferroelectrics*, **36**, 327–330.
Shen, X., Zhao, J., Wang, R., Yi, X., Yeh, P. & Chen, H. (1999). *Opt. Lett.* **24**, 312–314.
Tomita, Y., Bergquist, J. & Shibata, M. (1993). *J. Opt. Soc. Am. B*, **10**, 94–100.
Wolff, P. de (1974). *Acta Cryst.* A**30**, 777–785.
Woike, T., Petricek, V., Dusek, M., Hansen, N., Fertey, P., Lecomte, C., Arakcheeva, A., Chapuis, G. & Imlau, M. (2003). *Acta Cryst.* B**59**, 28–35.
Xia, H., Chen, H., Yu, H., Wang, K. & Zhao, B. (1998). *Phys. Status Solidus B*, **210**, 47–59.
Xu, Y. (1991). *Ferroelectric Materials and their Applications*. New York: Elsevier.
Xu, Y., Chen, H. & Cross, L. (1984). *Ferroelectrics*, **54**, 123–126.